2ème conférence Internationale des énergies renouvelables CIER-2014
Proceedings of Engineering and Technology - PET

2D simulation study of $In_{0.62}Ga_{0.38}N$ solar cell structure

A. Mesrane[a,*], F. Rahmoune[a], A. Oulebsir[a], A. Mahrane[b]
[a]University M'hamed Bougara of Boumerdes, LIMOSE laboratory, Boumerdes, Algeria
[b] Unité de Développement des Equipements Solaires, UDES/Centre de Développement des Energies Renouvelables (CDER), Route Nle n°11, BP386, 42415,Bou Ismaïl, Algeria
[*] mesranefatah@gmail.com

***Abstract*— The ability to tune the InGaN bandgap over a range providing a good spectral match to sunlight, makes it suitable for solar photovoltaic cells. The ultimate aim is to elaborate the most efficient solar cell made of multiple layers with different bandgaps. As a first step, the objective is to design the optimal InGaN single junction solar cell. Several models (the doping and temperature-dependent mobility model, Auger and Shockley-Read-Hall, the recombination model, the band gap narrowing model, the Fermi-Dirac statistics) were implemented in a two-dimensional numerical computer code (Atlas from Silvaco) in order to find the best configuration structure. Given that $In_{0.62}Ga_{0.38}N$ ($E_g = 1.39eV$) is the composition alloy that allows the best conversion efficiency for a single junction solar cell, the optimal structure found exhibits the following characteristics: J_{sc}=33.1149mA/cm^2, V_{oc}=1.0154 Volts, FF=88.3007 % and η =29.68 %.**

***Index Terms*— solar cell; InGaN; physical properties.**

1. INTRODUCTION

Recently, various studies of solar cells using III-nitrides semiconductors in the photovoltaic applications have been done. The InGaN alloy is a promising candidate for the photovoltaic applications because it exhibits attractive photovoltaic properties such as high tolerance to radiation, high mobility, and large absorption coefficient allowing thinner layers of material to absorb most of the solar spectrum [1].

Moreover, the InGaN alloys have a band gap energy which can be adjusted according to the Indium composition. Thus, the InGaN's energy band gap can be tuned from 0.7eV to 3.42eV, covering approximately the total solar spectrum.

It was shown theoretically that the band gap energy of about 1.39eV permits to achieve the maximum conversion efficiency [2], for a fraction composition of Indium of x=0.62 in the $In_xGa_{1-x}N$ alloy.

The objective of the work presented in this article is to study the $In_{0.62}Ga_{0.38}N$ p-n single-junction solar cell and extract the electrical parameters, such as the short circuit-current density (J_{sc}), the open-circuit voltage (V_{oc}), the fill factor (FF), the conversion efficiency (η), and to study their behavior for different doping concentrations and thicknesses of each layer of the device.

The effect of the temperature on the electrical characteristics of the $In_{0.62}Ga_{0.38}N$ single-junction solar cell have also been investigated.

2. MODELLING AND SIMULATION

2.1. Structure

As the numerical simulation is an important way to explore the possibility of new solar cell structure, the $In_{0.62}Ga_{0.38}N$ p-n single-junction solar cells has been studied using two-dimensional numerical computer simulation tool (ATLAS from Silvaco).

Atlas is a physically-based two and three dimensional device simulator. It predicts the electrical behavior of specified semiconductor structures [3].

To simplify the simulations, we have assumed that the reflections on the front face were negligible.

The $In_{0.62}Ga_{0.38}N$ single junction solar cell structure studied consists of a P-type emitter and N-type base, as shown in figure1:

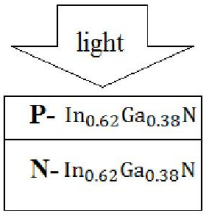

Figure 1. $In_{0.62}Ga_{0.38}N$ single junction solar cell structure

2.2. Physical models

The material used for our solar cell simulation consists of $In_{0.62}Ga_{0.38}N$ which has a band gap energy of 1.39eV. The band gap energy is related to the Indium composition fraction *x at a temperature of 300K* by [4]:

$$E_g(In_xGa_{1-x}N) = xEg_{InN} + (1-x)Eg_{GaN} - b.x.(1-x) \qquad (1)$$

where the band gap energy of InN (Eg_{InN}) and GaN (Eg_{GaN}) are 0.7eV and 3.42eV, respectively. x is the Indium content and b is the bowing parameter b=1.43.

The dependence of the energy band gap to the temperature is modeled in Atlas as follows [3]:

$$E_g(T_L) = E_{g300}(In_xGa_{1-x}N) + E_{g\alpha}\left[\frac{300^2}{300+E_{g\beta}} - \frac{T_L^2}{T_L+E_{g\beta}}\right] \quad (2)$$

where E_{g300} is given by the equation (1). $E_{g\alpha}$ and $E_{g\beta}$ are the parameters related to the materials used in the single junction. They are fixed respectively to $9.09\ x\ 10^{-4}\ eV.K^{-1}$ and $650\ eV.K^{-1}$ and are valid for the whole composition range of the $In_xGa_{1-x}N$.

The other modeling parameters of the $In_xGa_{1-x}N$ alloy were calculated using the following equations:

Electron affinity (χ) [5]:

$$\chi(In_xGa_{1-x}N) = 4.1 + 0.7(3.4 - Eg) \quad (3)$$

where Eg is the $In_xGa_{1-x}N$ band gap energy.

Relative permittivity (ε) [4]:

$$\varepsilon(In_xGa_{1-x}N) = 15.3x + 8.9(1-x) \quad (4)$$

Effective density of states in the conduction band (N_c) [5]:

$$Nc(In_xGa_{1-x}N) = \big(0.9x + 2.3(1-x)\big).10^{18} \quad (5)$$

Effective density of states in the valence band (N_v) [5]:

$$Nv(In_xGa_{1-x}N) = \big(5.3x + 1.8(1-x)\big).10^{19} \quad (6)$$

Effective masses (m_e/m_h) [3]:

$$m_e(In_xGa_{1-x}N) = 0.12x + 0.2(1-x) \quad (7)$$

$$m_h(In_xGa_{1-x}N) = 0.17x + 1.0(1-x) \quad (8)$$

The low field mobility model developed by M. Farahmand et al [6] has also been implemented in our model in order to study the hole and the electron mobilities behavior in the $In_xGa_{1-x}N$ alloy depending on the material composition and the temperature. The electron or hole mobility is given by the following expression:

$$U_0(N,T) = U_{min,i}\left(\frac{T}{300}\right)^{B1} + \frac{(U_{max,i}-U_{min,i})\left(\frac{T}{300}\right)^{B2}}{1+\left(\frac{N}{Nref\left(\frac{T}{300}\right)^{B3}}\right)^{\gamma\left(\frac{T}{300}\right)^{B4}}} \quad (9)$$

where T is the lattice temperature, N is the total doping of the layer, $Nref$ the doping of the substrate is fixed at $10^{17}\ cm^{-3}$, $B1, B2, B3, B4$ and γ are the specific parameters for a given material.

U_{min} and U_{max}, the values for the carrier mobilities, are given in the Table 1:

Table 1
Nitride Low Field Mobility Model Parameter Values [6]

Material	$U_{max,e}$ $(cm^2/V.s)$	$U_{min,e}$ $(cm^2/V.s)$
InN	3138.4	774
$In_{0.8}Ga_{0.2}N$	1252.7	644.3
$In_{0.5}Ga_{0.5}N$	758.1	459.4
$In_{0.2}Ga_{0.8}N$	684.2	389.4
GaN	1460.7	295

For other composition fractions not listed in Table 1, $In_xGa_{1-x}N$ electron mobilities were got by a linear interpolation from the nearest composition fractions. As the experimental data for the hole mobilities in the InGaN alloys are not available, we have assumed that the hole mobilities in the InGaN are the same as in the GaN [11].

The InGaN alloys absorption coefficients α is given by [7]:

$$\alpha(In_xGa_{1-x}N) = 10^5\sqrt{C\big(E_{ph} - E_g\big) + D\big(E_{ph} - E_g\big)^2} \quad (10)$$

where E_{ph} and E_g are the photon energy and the band gap energy of $In_xGa_{1-x}N$, respectively. C and D are parameters dependent on the alloy composition.

Table 2
Fitting parameters used to calculate the absorption coefficient of the $In_xGa_{1-x}N$ alloys [7]

Indium composition	C	D
1	0.69642	0.46055
0.83	0.66796	0.68886
0.69	0.58108	0.66902
0.57	0.60946	0.62182
0.5	0.51672	0.46836
0	3.52517	-0.65710

For the $In_xGa_{1-x}N$ alloys, the Adachi's wavelength-dependent refractive index model is given by the following equation [8]:

$$n(E) = \sqrt{A\left(\frac{E_{ph}}{E_g}\right)^{-2}\left\{2 - \sqrt{1+\frac{E_{ph}}{E_g}} - \sqrt{1-\frac{E_{ph}}{E_g}}\right\} + B} \quad (11)$$

where A and B depend on the material composition. In the case of the $In_xGa_{1-x}N$ alloy, A and B are given by the following equation [8]:

$$A(In_xGa_{1-x}N) = 13.55x + 9.31(1-x) \quad (12)$$

$$B(In_xGa_{1-x}N) = 02.05x + 3.03(1-x) \quad (13)$$

Some assumptions have been adopted to simplify the simulations. Thus, the minority carrier lifetime for the electrons and holes are assumed to be the same ($\tau_{e,h} = 6.5\ ns$) [9]. The Auger recombination coefficients for the electrons and the holes, for the $In_xGa_{1-x}N$ alloys, are set at ($1.5x10^{-30} cm^6.s^{-1}$)[10]. The surface recombination velocities of the minorities (electrons or holes) were assumed to be $10^3 cm/s$ [9].

In order to take into account the action of several physical phenomena that take place in the structure, the following physical models have been implemented:

- The band gap narrowing effects.
- The doping and temperature-dependent mobility models.
- The Auger recombination models.
- The Schokly-Read-Hall recombination models.
- The Fermi-Dirac statistics.

3. RESULTS AND DISCUSSION

In order to get the best $In_{0.62}Ga_{0.38}N$ single-junction solar cell configuration, a great number of simulations were done to select the optimal device parameters as the optimal doping concentration, the optimal thickness of the front layer.

3.1. Optimal doping concentrations of the front layer

With a known proper total thickness of $In_{0.62}Ga_{0.38}N$ SJ solar cell, we have calculated the conversion efficiency for various values of the acceptor doping concentrations Na. (donors concentration Nd is assumed to be the same with Na).

The solar cell efficiency is given by:

$$\eta(\%) = \frac{Isc.Voc.FF}{Pin} \qquad (14)$$

where Isc is the short circuit current, Voc is the open circuit voltage, FF is the fill factor, and Pin is the incident power of the solar spectrum.

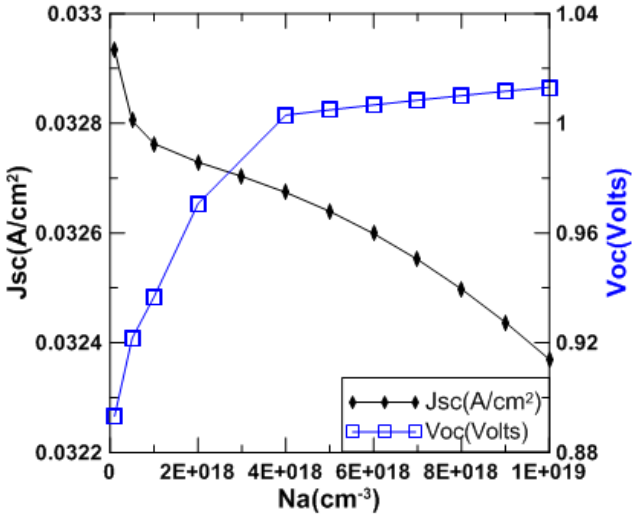

Figure 2. The short circuit current density and the open circuit voltage versus the doping concentration Na.

As the doping concentration $N_i (i = A \text{ or } D)$ decreases, the carrier mobility and the minority carrier lifetime increase, inducing an enhancement in the minority carrier diffusion length, and a better collection efficiency, resulting in the improvement of the current density.

The open circuit voltage of the p-n junction solar cell is given by the following equations:

$$Voc = \frac{K_B.T}{q} \ln\left(\frac{J_{sc}}{J_0} + 1\right) \qquad (15)$$

$$J_0 = q.n_i^2 \left(\frac{D_e}{L_e N_A} + \frac{D_h}{L_h N_d}\right) \qquad (16)$$

where K_B and q are Boltzmann's constant and electron charge, respectively. $D_{e,h}$ and $L_{e,h}$ are respectively the diffusion constants and the diffusion lengths of the minority carrier (electron and hole). J_0 is the reverse saturation current density and n_i is the intrinsic carrier concentration.

According to the equations (15,16), the open circuit voltage increases when the doping concentration increases.

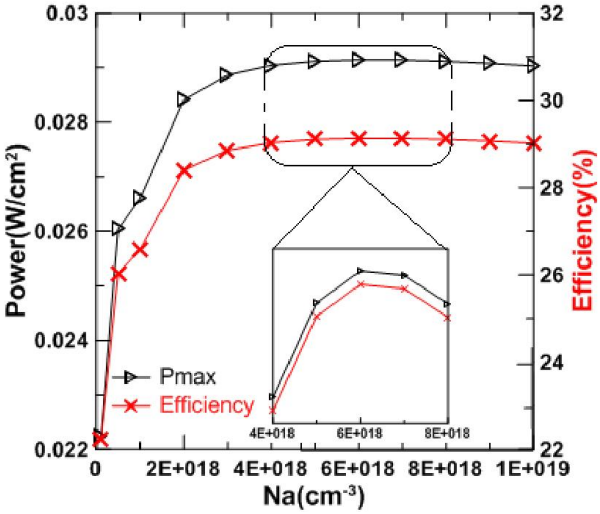

Figure 3. The Maximal power and the solar efficiency of the solar junction versus the doping concentration Na.

As shown in figure 3, while the doping concentration Na increases, the maximal power produced by the solar cell and its conversion efficiency increase first and then decrease.
The optimum efficiency of $In_xGa_{1-x}N$ single-junction solar cell was reached when the doping concentrations were both $(6.10^{18} cm^{-3})$.

3.2. Optimal thickness of the front layer

Since the optimal doping concentration was found, the main parameters of the $In_{0.62}Ga_{0.38}N$ single-junction solar cell such as $J_{sc}, V_{oc}, P_{max}, FF and$ η , were calculated for a range of p-layer thicknesses comprised between 0.01 µm to 1µm.

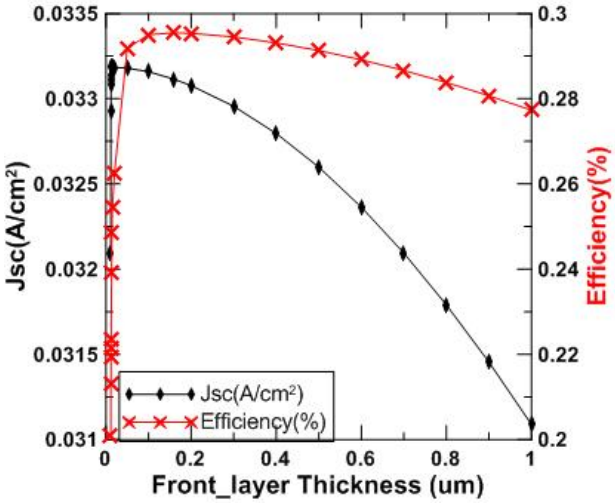

Figure 4. Calculated efficiency η and short circuit current density J_{sc} versus the front layer thickness.

As shown in figure 4, the conversion efficiency and the short circuit current density increase, first, sharply with the increasing of the front layer thickness, and then decrease.

When the front layer thickness decreases, the distance between the space charge region and the surface decreases, that improves the effective collection efficiency inducing the enhancement of the short circuit current density. In the same time the collection efficiency of the space charge region will be weakened as this last is too close to the surface if the surface recombination was considered. The reduction of the collection efficiency leads to the decrease of the short circuit current. It was found that the best efficiency was reached for a front layer thickness of 0.16µm.

3.3. Optimal performance of $In_{0.62}Ga_{0.38}N$ SJ solar cell

The optimal performance of $In_{0.62}Ga_{0.38}N$ single-junction solar cell was found for 0.16µm p-layer thickness and 0.5µm n-layer thickness, with $6.10^{18}cm^{-3}$ doping concentrations for both regions.

Table 3
Calculated parameters of the $In_{0.62}Ga_{0.38}N$ SJ solar cell under AM1.5G, 0.1W/cm^2 and 300K.

PV parameters	values
$J_{sc}(mA/cm^2)$	33.1149
V_{oc}(Volts)	1.0154
$P_{max}(mW/cm^2)$	29.6910
$FF(\%)$	88.3007
η(%)	29.68

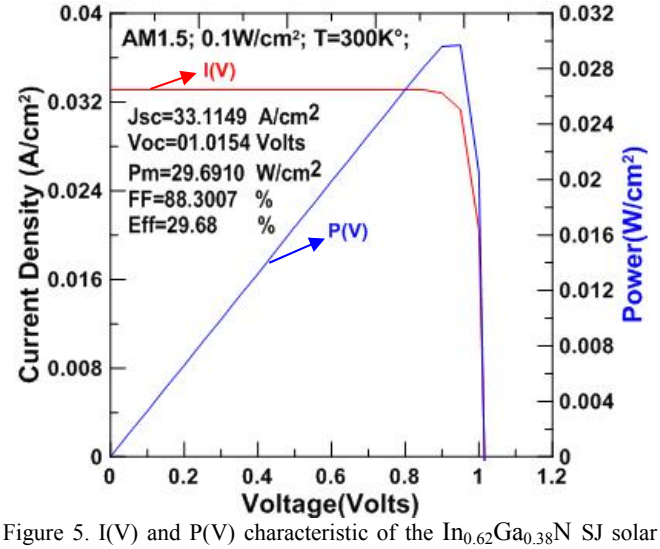

Figure 5. I(V) and P(V) characteristic of the $In_{0.62}Ga_{0.38}N$ SJ solar cell with the optimum performance.

3.4. The temperature dependence of $In_{0.62}Ga_{0.38}N$ SJ solar cell

The photovoltaic parameters of the $In_{0.62}Ga_{0.38}N$ SJ solar cell were calculated for different values of temperature in order to understand the electrical behavior of the solar cell under high temperatures.

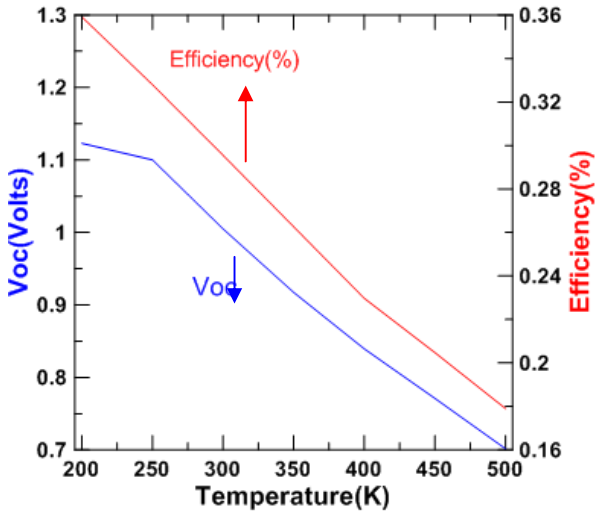

Figure 6. Efficiency and open circuit voltage as a function of temperature for $In_{0.62}Ga_{0.38}N$ SJ solar cell.

As shown in Figure 6, the open circuit voltage, and the efficiency was highly degraded with the increasing of temperature.

The open circuit voltage decreased with the increased temperature due to the reduction of the band gap energy and the extremely increased reverse saturation current, which is very sensitive with temperature, inducing the degradation of the solar efficiency.

4. CONCLUSION

The calculation of the photovoltaic parameters of the $In_{0.62}Ga_{0.38}N$ p-n single junction solar cell, for the cases of different doping concentrations and different thicknesses of each layers, has allowed to achieve the best solar cell structure with optimum performances.

The optimum efficiency, found under normalized conditions (AM1.5G, 0.1 W/cm^2, and 300°K), is 29.68%. The performances of the solar cell vary with the temperature. We noticed efficiency degradation with the increasing of the temperature, this is due to the temperature dependency of the physical parameters of the solar cell.

REFERENCES

[1] L.A. Vilbois, A. Cheknane, A. Bensaoula, C. Boney, T. Benouaz, "Simulation of a solar cell based on InGaN", Energy Procedia, vol.18, pp 795-806, 2012.

[2] T.Zdanowicz, T. Rodziewicz, M. Zabkowska-Waclawek,"Theoretical analysis of the optimum energy band gap of semiconductors for fabrication of solar cells for applications in higher latitudes locations", Solar Energy Materials and Solar Cells, vol.87, pp 757-769, May 2005.

[3] Silvaco data system Inc 2013 atlas user's manual Ver 5.14.0.R.

[4] Muhammad Nawaz and Ashfaq Ahmad, "A TCAD-based modeling of GaN/InGaN/Si solar cells", Semicond. *Sci. Technol.* 27 035019, 2012.

[5] Dennai Benmoussa, Benslimane Hassane and Helmaoui Abderrachid, "Simulation of In0.52Ga0.48N solar cell using AMPS-1D", Renewable and Sustainable Energy Conference (IRSEC), 2013 International, pp 23-26, 2013.

[6] Farahmand, M. **,** Garetto, Carlo **,**Bellotti, E. **,** Brennan, Kevin F. **,** Goano, M. **,** Ghillino, E. **,** Ghione, G. **,** Albrecht, J.D. **,** Ruden, P.Paul , "Monte Carlo simulation of electron transport in the III-nitride wurtzite phase materials system: binaries and ternaries", Electron Devices, IEEE Transactions on**, V**ol**.** 48 , Issue: 3 , pp 535 – 542, 2001.

[7] G.F. Brown , J.W. Ager III, W. Walukiewicz, J.W,"Finite element simulations of compositionally graded InGaN solar cells", Solar Energy Materials & Solar Cells, Vol. 94, pp 478–483, 2010.

[8] Piprek, J., Semiconductor Optoelectronic Devices: Introduction to Physics and Simulation. UCSB: Academic Press 2003.

[9] Xiaobin Zhang, Xiaoliang Wang, Hongling Xiao, Cuibai Yang, Junxue Ran, Cuimei Wang, Qifeng Hou and Jinmin Li,"Simulation of In0.65Ga0.35N single-junction solar cell", J. Phys. D: Appl. Phys. Vol. 40,pp 7335–7338, 2007.

[10] Jani O K ,"development of wide-band gap InGaN solar cells for high-efficiency photovoltaics", phD Thesis, Georgia Institute of Technology August, 2008.

[11] F.Bouzid and L.Hamlaoui, "Investigation of InGaN/Si double junction tandem solar cells", J. Fund. App. Sci., Vol. 4, pp 59–71, 2012.